Turkish Journal of Electrical Engineering & Computer Sciences

http://journals.tubitak.gov.tr/elektrik/

Research Article

Turk J Elec Eng & Comp Sci
(2018) 26: 150 – 161
© TÜBİTAK
doi:10.3906/elk-1608-50

An efficient algorithm to decompose a compound rectilinear shape into simple rectilinear shapes

Imran SHARIF[1,*], Debasis CHAUDHURI[2], Naveen Kumar KUSHWAHA[1], Ashok SAMAL[3], Brij Mohan SINGH[4]

[1]Image Analysis Center, DEAL, DRDO, Dehradun, Uttarakhand, India
[2]DRDO Integration Center Ministry of Defence, Panagarh, West Bengal, India
[3]Department of Computer Science and Engineering, University of Nebraska-Lincoln, Lincoln, NE, USA
[4]Department of Information Technology, COER, Roorkee, Uttarakhand, India

Received: 05.08.2016 • **Accepted/Published Online:** 12.11.2017 • **Final Version:** 26.01.2018

Abstract: Detection of a compound object is a critical problem in target recognition. For example, buildings form an important class of shapes whose recognition is important in many remote sensing based applications. Due to the coarse resolution of imaging sensors, adjacent buildings in the scenes appear as a single compound shape object. These compound objects can be represented as the union of a set of disjoint rectilinear shaped objects. Separating the individual buildings from the resulting compound objects in a segmented image is often difficult but important nevertheless. In this paper we propose a new and efficient technique to decompose a compound shape into a set of simple rectilinear shapes. First, the true interior and exterior corner points of the compound object are extracted. A modified corner detector based on polygonal approximation is proposed to accurately determine the boundaries of compound shapes. The compound shape is then split at the interior corner points to minimize the difference between the perimeter of the compound object and the sum of the perimeters of the decomposed objects. We have systematically compared the results our algorithm with those of existing approaches and the results show that the proposed algorithm is more accurate than the algorithms in the literature in terms of accuracy of perimeter estimation and computational cost.

Key words: Compound object, pattern recognition, feature extraction, corner point detection, shape analysis, building extraction

1. Introduction

Decomposition is a technique used to split complex structures into smaller, simpler, and more manageable units. Shape decomposition is a common and important problem in digital image processing and pictorial pattern recognition. It provides descriptions of objects using their constituent shapes, which can then be used for object recognition. Buildings in remotely sensed imagery are unique composite shapes and their detection is important in various civilian and military applications. Due to their spatial proximity, many buildings form L-shaped, U-shaped, or even more complex compound patterns in low resolution remotely sensed images. In such situations, it is difficult to extract the individual objects directly without a decomposition step. An efficient decomposition algorithm must divide an irregular pattern of objects (e.g., merged building footprints) into a set of regular rectilinear shaped objects.

Zakaria et al. [1] have proposed an image decomposition technique to speed up the moment calculation,

*Correspondence: imran_ietk@rediffmail.com

which is a *delta* method and decomposed the object into individual rows of pixels. Spiliotis and Mertzios [2] proposed a simple but significant improvement to the delta method. This generalized delta-method (GDM) uses a rectangular-wise object representation instead of the row-wise one. A popular hierarchical decomposition scheme, quad tree decomposition (QTD), is used for representation and compression [3]. Graph-based decomposition (GBD) is another popular decomposition approach and is widely proposed [4]. Zhang and Lu [5] have summarized a number of techniques for shape representation and decomposition. Wang et al. [6] proposed a new decomposition and modeling method to reconstruct a compound building from LiDAR data and aerial imagery; it is based on the idea that a compound building can be decomposed into a set of primitives that can also be reconstructed by using the primitives. Har-Peled and Roy [7] proposed an algorithm that determines the maximum possible overlap of two polygons under translation by decomposing them into convex parts. Nagamochi and Abe [8] proposed a technique to decompose a rectangle into $n$rectangles so that the set of resulting rectangles can minimize an objective function such as the sum of perimeters of the rectangles, the maximum perimeter, and the maximum aspect ratio of the rectangles.

Decomposition techniques have also been proposed in a number of other contexts as well. Recently, Liu et al. [9] proposed a dual space decomposition technique that handles complex 2D shapes with a hole recognition step and further labeled each hole either as a noise or an important structural feature.

The rest of the paper is organized as follows. The proposed interior corner point detection approach is described in Section 2. Section 3 presents the modified corner detector algorithm that is robust in the presence of distortion of the edges at the object boundary and the proposed decomposition technique. The experimental results and discussion are presented in Section 4. Finally, a summary and directions for future research are presented in Section 5.

2. Interior corner point detection

Corners and other high curvature points are widely used in shape descriptions since it is

thought that they have high information content. Many algorithms for detecting the corners are available in the literature [10].

The Sojka corner detection algorithm [11], based on measuring the variance of the directions of the brightness gradients, has been used in this research. The probability of a set of image points approximating straight segments that intersect at a possible corner point is determined using a Bayesian approach. This information is then used to compute the angle between the intersecting segments. The interested reader is referred to [11] for its underlying theoretical foundation and additional details. We propose a template-based interior corner point detection algorithm to filter out the exterior corner points, which is described next.

2.1. Template-based interior corner detector

A template-based approach used to detect the interior corner points of an object is shown in Figure 1. Here assume that a black pixel (1) represents the foreground/object and a white pixel (0) corresponds to the background. If a pixel is an interior corner point then 0 pixel value of the 2 $\times$ 2 templates is placed in the position of candidate pixel. If any of the templates match at a pixel then it is labeled as an interior corner point. Template-based interior corner point detectors work best when the boundaries of the object are horizontal or vertical and are free of distortion of the edges.

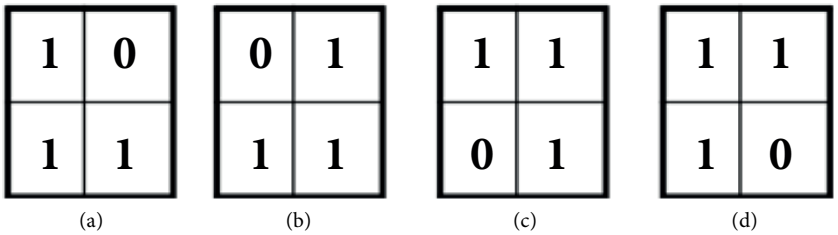

Figure 1. The four templates for interior corner point detection.

2.2. True interior corner point detector (TICPD)

Some mathematical definitions used in the true interior corner detection (TICPD) algorithm are first presented.

Definition 1 *The set of interior and exterior corner points is denoted by* C_{IE} .

Definition 2 *The set of all corner points of an object as detected by the template-based interior corner point detector is the interior corner points set and is denoted by* C_I .

Definition 3 *The set of real interior corner points of an object is the true interior corner points set, which is obtained by the TICPD algorithm, and is denoted by* C_{TI} .

Definition 4 *The distance between the two points* $C[i]$ *and* $C[i-1]$ *is denoted as* $d_{i,i-1}$.

TICPD Algorithm

Step 1: Find the corner points set, C_{IE}, using the Sojka corner detection algorithm [11].
Step 2: Find the interior corner points set, C_I using the template-based interior corner detection algorithm.
Step 3: Find the true interior corner points C_{TI}, as the intersection of C_{IE} and C_I i.e. $C_{TI} = C_{IE} \cap C_I$.

3. Compound polygon decomposition technique

The objective of polygon decomposition is to divide a given convex/concave polygon into a minimal set of predefined primitives. L-patterns or U-patterns or compound rectangles are also convex or concave polygons and decomposition of such polygons into a minimal set of disjoint rectilinear shape objects is the focus of this paper. The approach proposed in this paper is based on a heuristic search, where the objective function to be minimized is the difference between the perimeter of the compound object and the sum of the perimeters of the decomposed objects. The schematic of the algorithm is given in Figure 2. The algorithm begins with the set of interior corner points derived using the TICPD algorithm (Section 2). The major steps in the decomposition algorithm are as follows:

1. Arrange the corner points set C_{IE} along the boundary in a clockwise direction
2. Identify the interior corner points C_I as the candidate points for decomposition and its two adjacent corner points for finding the directions of decomposition

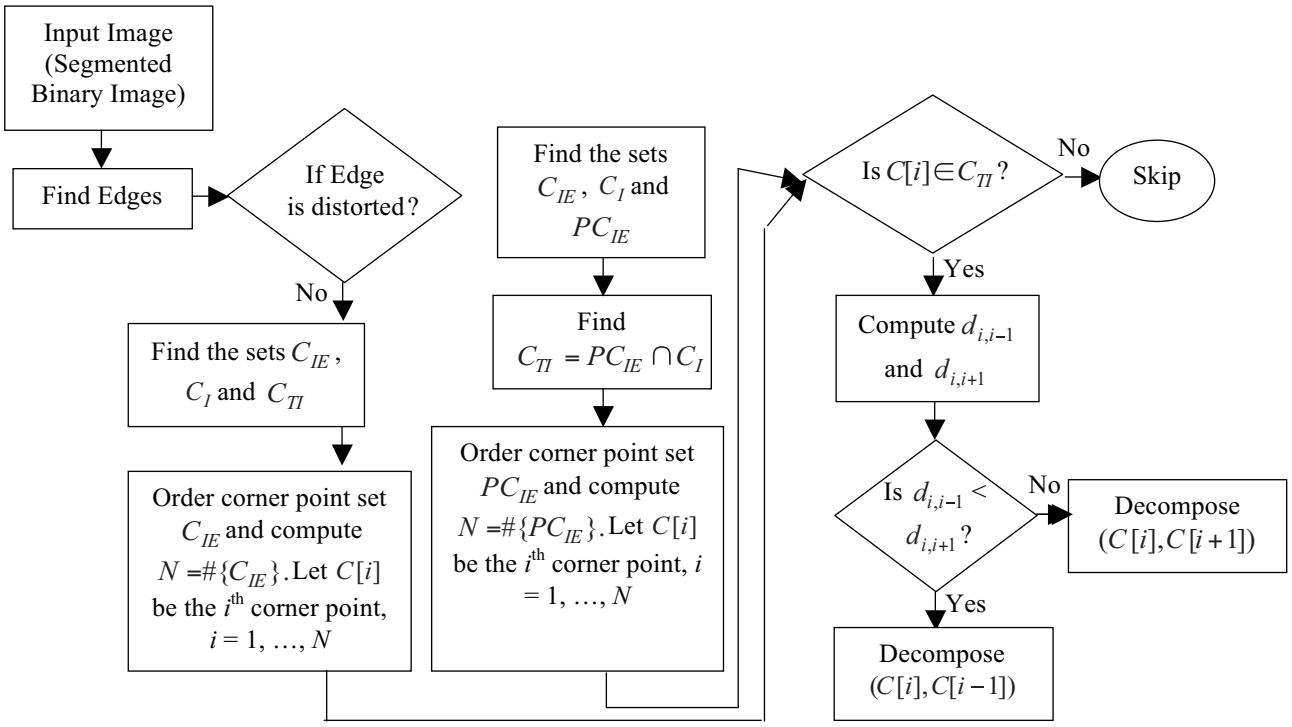

Figure 2. Overall schematic of the algorithm.

3. Decompose the compound object from interior corner point along the opposite direction of the adjacent corner point that leads to the shortest distance to the boundary. In order to derive a sequential arrangement of the corner points, the Moore neighborhood tracing algorithm has been used in this paper. Some mathematical definitions used in the proposed decomposition technique are introduced next.

Definition 5 *A set of rectilinear shape objects S is a partition of a compound rectilinear shape object F, if $\bigcup_{A \in S} A = F$ and $\underset{A,B \in S}{\forall} A \neq B \Rightarrow A \cap B = X$, where $X = \varphi$ or $X \subseteq$ Boundary$(A) \cup$ Boundary(B), i.e. the intersection of A and B may only contain the boundary points of A or B.*

Definition 6 *The set of all corner points of a polygon in the form of a sequential order in clockwise direction is called an ordered corner point set and is denoted by O_C.*

Definition 7 *An ordered neighborhood of a corner point $X_i \in O_C$ is given by $ON(X_i) = (X_{i-1}, X_i, X_{i+1})$, where $X_{i-1} \in O_C$ is a corner point that appears before X_i in O_C and $X_{i+1} \in O_C$ is a corner point that appears before X_i in O_C. The two corner points X_{i-1} and X_{i+1} are called the preposition corner point and postposition corner point, respectively, with respect to X_i.*

Definition 8 *Let $(X_{i-1}, X_i, X_{i+1}) \in O_C$ be an ordered neighborhood for a corner point X_i. Boundary connector segments for corner X_i are defined by the line segments from X_i to the border of the object in the direction opposite the segments $\overrightarrow{X_i X_{i-1}}$ and $\overrightarrow{X_i X_{i+1}}$ defined by the points $\overrightarrow{B_{i-1}}$ and $\overrightarrow{B_{i+1}}$, respectively. The edge weights of these boundary connector segments are denoted by $d_{i,i-1} = d(X_i, X_{i-1})$ and $d_{i,i+1} = d(X_i, X_{i+1})$, respectively. The edge weight is calculated by the Euclidean distance between the two points.*

Definition 9 *The main axis of an object is defined by the line that connects the two furthest points in the object.*

The decomposition of the compound polygon ABCDEFGH shown in Figure 3a, using the proposed algorithm, is briefly explained next. In this example, the set of corner points (both exterior and interior) and the set of true interior corner points are $C_{IE} = \{A, B, C, D, E, F, G, H\}$ and $C_{TI} = \{D, E\}$, respectively. An ordered corner point set of the compound polygon, O_C , is {A,B,C,D,E,F,G,H}. The ordered neighborhoods of the two true interior corner points {D,E} are given by the triplets $(C, D, E) \in O_C$ and $(D, E, F) \in O_C$, respectively. For each interior corner point, there are two boundary-connected segments, the minimum and the maximum as defined earlier (Definition 8). These travel paths are in the directions opposite to the directions between the interior corner point and the two neighboring corners. Two paths for the corner C are shown in Figures 3b and 3c. For each of the two cases, we can also identify the two corresponding minimum and maximum boundary connected segments as shown in Figures 3d– 3g. Thus, in this example, Figure 3d represents the smaller difference of the perimeters of the compound rectilinear shape object and the sum of the perimeters of the simple decomposed rectilinear shape objects. It should be noted that the decomposition technique is dependent on the first interior corner point of the ordered corner point set O_C. As a result, the representation of union of disjoint rectilinear shape objects of the compound rectilinear shape object may not be unique due to rotation of the object. To overcome this problem, we propose to use the closest corner (in clockwise direction) from the end point of the main axis (Definition 9) of the object as the starting point. With this addition, the decomposition is invariant under translation, rotation, and scaling. Moreover, the difference between the perimeter of the compound rectilinear shape object and the sum of the perimeters of the simple rectilinear shape objects is small. This mathematical concept has been informally demonstrated below through the following proposition.

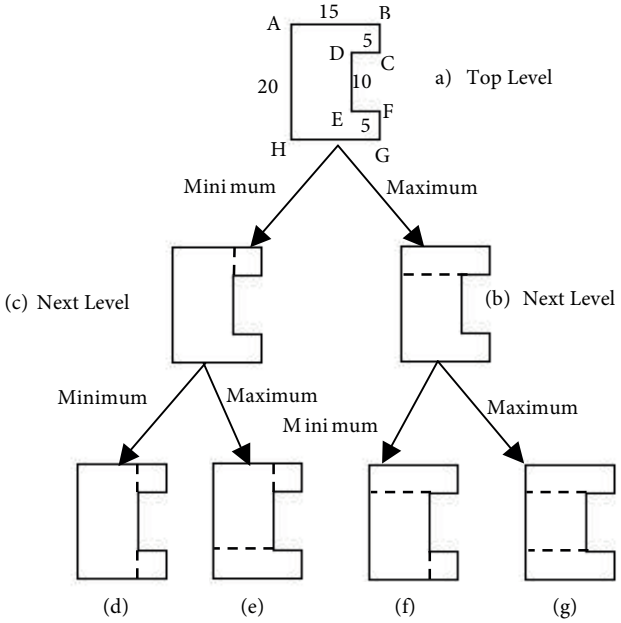

Figure 3. Different combinations of decomposition states based on segment lengths.

Proposition 1 *Let P_0 be the length of the perimeter of the compound rectilinear shape object. Let $P_{\min}$ and $P_{\max}$ be the sum of the perimeters of the rectilinear shape objects derived using the minimum and maximum straight travel paths (as definition 8) during decomposition, respectively. Then $|P_0 - P_{\min}| \leq |P_0 - P_{\max}|$.*

Proof Let S be the compound rectilinear shape object in which $C_{IE} = \{A, B, C, D, E, F\}$ and $C_{TI} = \{E\}$ (as shown in Figure 4). Now $ON(E) = \{F, E, D\}$ (Definition 7) and the decomposition takes place at $E \in C_{TI}$ along the opposite direction of either $\overline{EF}$ or $\overline{ED}$. It is always true that $P_{new} = P_0 + 2\times$ Length of the connecting segments, due to decomposition at E.

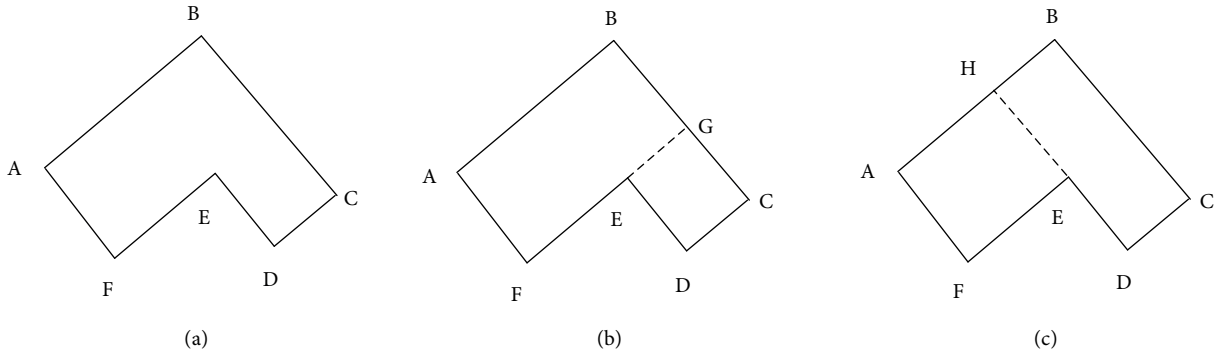

Figure 4. Decomposition of a) compound rectangle, b) along minimum, and c) maximum travel path.

Furthermore, by definition, $P_{\min} \leq P_{\max}$, since the length of the connecting segment (EG) due to minimum travel path $\leq$ length of the connecting segment (EH) due to maximum travel path. Since P_0 is fixed for a particular compound rectilinear shape object, it follows that $|P_0 - P_{\min}| \leq |P_0 - P_{\max}|$. □

The main drawback of the proposed decomposition technique is that when the boundary of the object is degraded by distortion of edges, the result is not accurate. To overcome this, an additional step has been proposed to make the corner point detection more robust. When the boundary is distorted, a polygonal approximation on the set of corner points can first be derived and the corner points of the polygon can be used as C_{IE}. Polygonal approximations can avoid small spurious lines/distortion in the contour, making the feature extraction phase more accurate [12]. This can subsequently improve the performance of any shape analysis performed downstream. For this research, we have used the algorithm proposed by Chaudhuri and Kushwaha [13], a nonparametric method for automatic threshold selection of such iterative endpoint fit algorithm. The algorithm is effective in shape analysis, where the polygonal approximation must maintain the relative levels of detail present in the contour while capturing the outline of the shape. The modified corner point detection algorithm is given below.

4. Modified corner point detector (MCPD)

Step 1: Apply Sojka corner point detector algorithm and find the set C_{IE}.
Step 2: Apply template-based interior corner point detector algorithm and find the set C_I.
Step 3: Find polygonal approximation of the corner points set, C_{IE}. Let PC_{IE} be the set of corner points of the polygonal approximation. Find the vertices of the polygonal approximation, which are the modified corner points set, $PC_{IE} \subseteq C_{IE}$.
Step 4: Find the true interior corner points as the set C_{TI}, which is the intersection of PC_{IE} and C_I, i.e. $C_{TI} = PC_{IE} \cap C_I$.

Now the overall decomposition algorithm is formally given below

Algorithm 1 Decompose Compound Rectangle

Input $\rightarrow I$: Binary image, I
Output $\rightarrow D$: Decomposed image, D
C_{IE} = Sojka Corner Detector (I); // Corner points (interior and exterior)
C_I = Template Based Interior Corner Detector (I); // Interior corner points
E = Find edge of the binary image (I);
if (E is distorted edges) {
    Find PC_{IE}
    $C_{TI} = PC_{IE} \cap C_I$ // True interior corner points from MCPD }
else
$C_{TI} = C_{IE} \cap C_I$ // True interior corner points from TICPD
$N = \#\{C_{TI}\}$
C = Ordered Corner Point Set (C_{IE}); // $C[i]$ is the i'th corner point, $i = 1, ..., N$
For $i = 1, ..., N$
    if $(C[i] \notin C_{TI})$ skip; // C[i] is not an interior corner point
$d_{i,i-1} = d(C[i-1], C[i])$; // distance between $C[i]$ to boundary point opposite to $C[i-1]$
$d_{i,i+1} = d(C[i+1], C[i])$; // distance between $C[i]$ to boundary point opposite $C[i+1]$
  if $d_{i,i-1} < d_{i,i+1}$
      Decompose($C[i]$, $C[i-1]$) // from C[i] to the border opposite to C[i – 1]
    else
      Decompose($C[i]$, $C[i+1]$) // from C[i] to the border opposite to C[i + 1]
end

It can be seen that the computational complexity of the algorithm is $O(p \times q)$, where p and q are the numbers of true interior and exterior points of the object.

5. Experimental results and discussion

We have demonstrated the effectiveness of the proposed algorithm using (a) an synthetic image, (b) a QuickBird satellite image, and (c) ISPRS benchmark dataset of the city of Vaihingen (Germany).

Synthetic Images: Figures 5a and 5c show the same compound rectilinear shape object formed by eight distinct nonoverlapping rectilinear shapes in different orientations. In Figure 5a the boundary segments of the rectilinear objects are aligned with either the horizontal or the vertical axes. On the other hand, all boundaries of the object in Figure 5c are inclined with respect to both the horizontal and vertical axes. The proposed decomposition algorithm generates the same set of simple rectilinear shape objects as shown in Figure 5b and Figure 5d. This shows that the proposed decomposition technique is invariant under rotation. Furthermore, the proposed algorithm extracts all eight rectilinear shapes of the compound rectilinear object accurately.

Quick Bird Images: An original Quick Bird panchromatic image (taken from [14]) is shown in Figure 6a. The corresponding segmented image is shown in Figure 6b. Figure 6d shows the interior corner points (a total of 44) obtained using the template- based interior corner detector. The true interior corner points (only 5) identified by the TICPD algorithm are shown in Figure 6e.

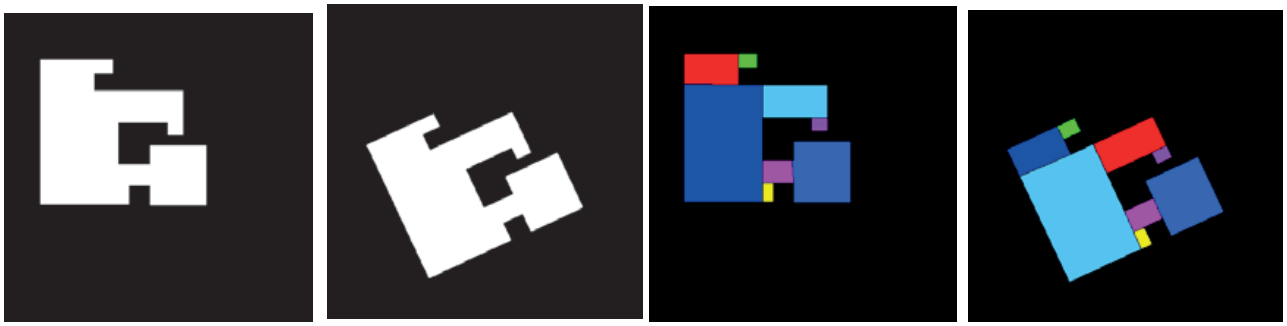

(a) (b) (c) (d)

Figure 5. Object in which the axes are a) parallel and b) nonparallel to horizontal and vertical axes, c) Decomposed rectilinear shape objects by the proposed decomposition technique of first object and d) second object.

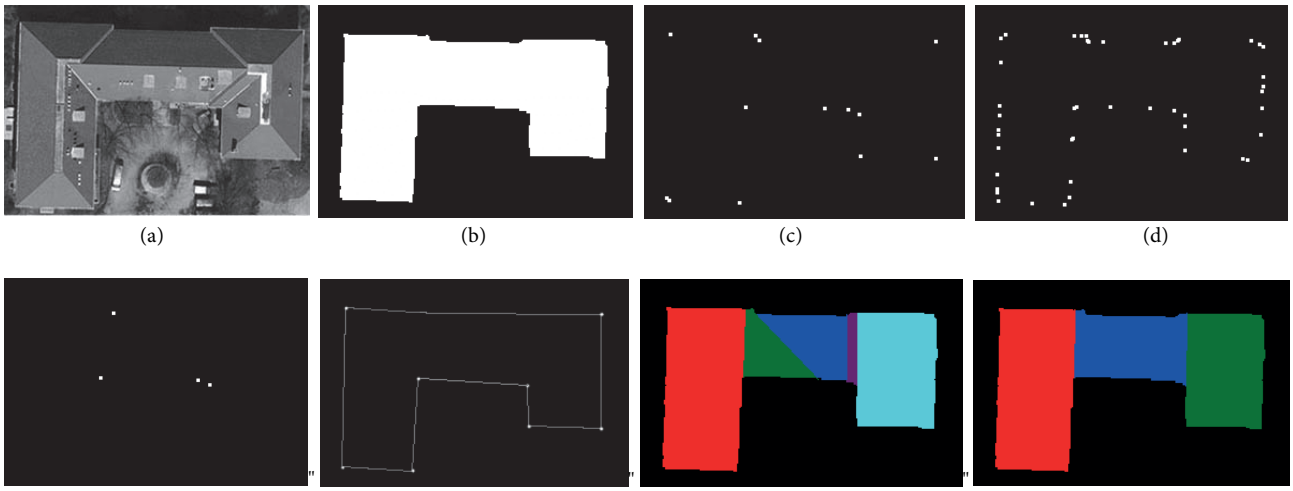

(a) (b) (c) (d)

(e) (f) (g) (h)

Figure 6. Decomposition of an object in remote sensing data: a) original panchromatic QuickBird satellite image, b) segmented image, c) corner points by Sojka algorithm [11], d) interior corner points using template-based operator, e) interior corner points using proposed TICPD algorithm, f) polygonal approximation and detected corner points, which are vertices of the polygon, g) decomposed objects by the proposed decomposition technique using nonpolygonal and h) polygonal approximation.

As discussed before, due to the nature of satellite imagery, boundaries of polygonal objects do not appear perfectly linear, resulting in spurious corner points and the decomposition algorithm generates the rectilinear shapes as shown in Figure 6g. To overcome this problem, the modified corner detector algorithm using polygonal approximation has been applied. The polygonal approximation of the object and the corner points (only two interior corner points), which are the vertices of the fitted polygon, are shown in Figure 6f. As can be clearly seen, many unwanted corner points detected by the Sojka corner point detector are eliminated by using the modified corner point detector. The compound region in Figure 6b is the union of three rectilinear shapes and the three shapes are correctly identified by the proposed modified decomposition technique as shown in Figure 6h. In contrast, the TICPD algorithm incorrectly detects four rectilinear shape objects, as shown in Figure 6g. This shows the efficacy of the modified corner point detector for objects with noisy boundaries. Although the building in Figure 6a is a single object, the proposed technique breaks the compound rectilinear shape into

disjoint rectilinear shapes. This is a problem in the detection of buildings from remotely sensed imagery, where one needs to consider the homogeneity of the polygon to decide if it should be divided. This is not an issue in this paper, however.

Even though the focus of the present paper is not on building detection from aerial/satellite images, we use the ISPRS benchmarking datasets to examine the performance of the proposed technique for decomposing both densely and sparsely populated buildings. Rottensteiner et al. [15] have proposed several methods in the literature for urban area extraction and they were compared based on the benchmark dataset. Figure 7 shows Vaihingen (Germany) city image, which a subset used for the test of digital aerial cameras carried out by the German Association of Photogrammetry, Remote Sensing and Geoinformation (DGPF) [15,16]. The original image is a 16-bit pan-sharpened color infrared image with a ground resolution of 8 cm. Figures 7b and 7c show the images of Area 1 and Area 2 of the image, respectively. Area 1 has densely populated buildings with

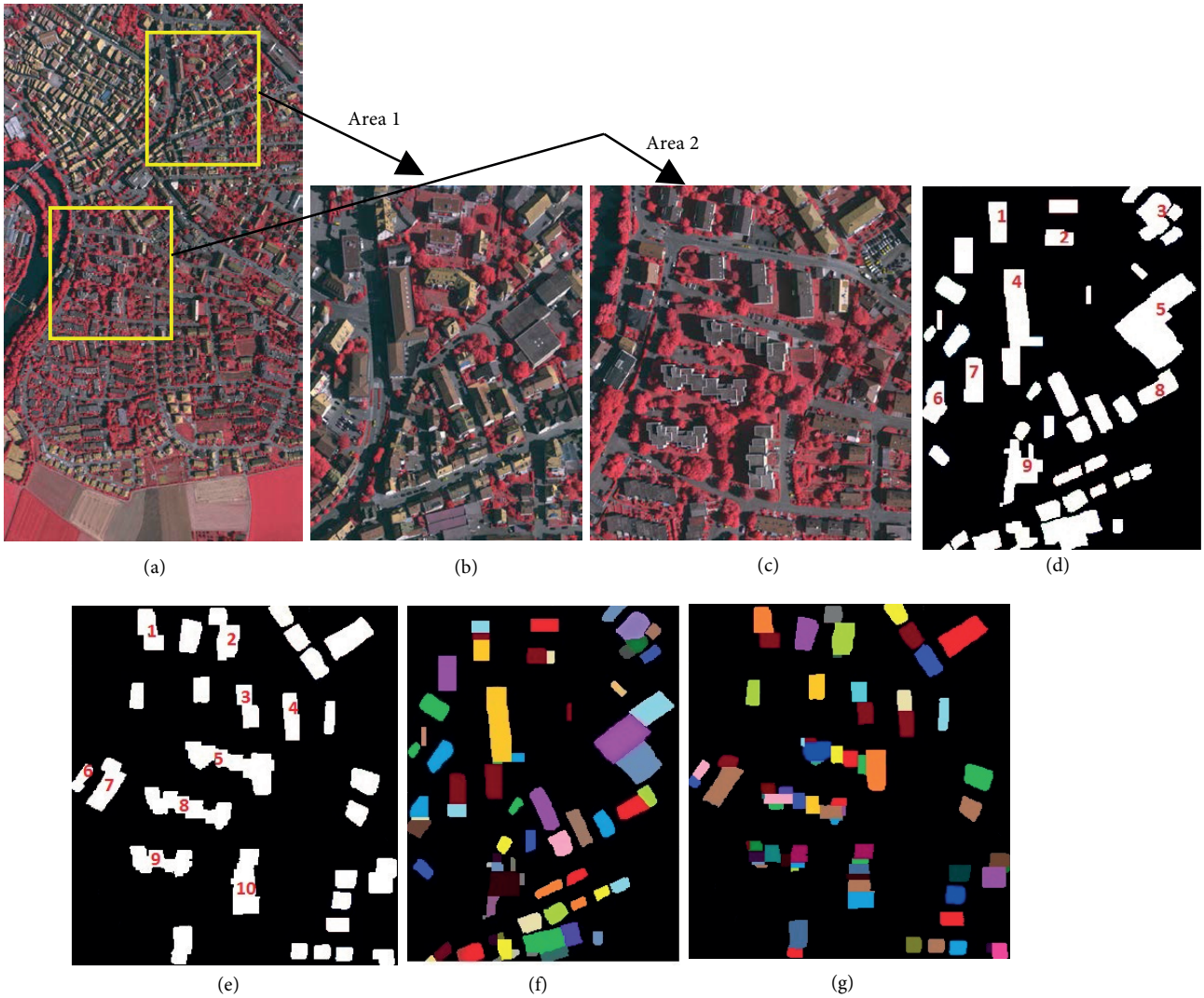

Figure 7. Vaihingen city test areas: a) original image, b) Area 1, c) Area 2, d) segmented image of Area 1 and e) Area 2, f) decomposed rectilinear objects of Area 1 and g) Area 2 by the proposed technique.

complex shapes, roads, and trees. Area 2, in contrast, consists of a few high rise residential buildings surrounded by trees. The buildings detected by the algorithm proposed by Chaudhuri et al. [17] for Area 1 and Area 2 are shown in Figures 7d and 7e, respectively. Figures 7f and 7g show the decomposed rectilinear shapes derived by the proposed decomposition algorithm. It can be observed that most compound rectilinear shape objects (multiple objects in both Scenes 1 and 2) are correctly decomposed by the proposed decomposition algorithm.

Now we compare the performance of our decomposition technique with other methods proposed in the literature. We use an image of size 512 $\times$ 512 with a compound rectilinear shaped object as shown in Figure 8a. The results of decomposition by GDM [2], GBD [4], QTD [3], and the proposed decomposition techniques are shown in Figures 8b–8e, respectively. Most of the papers have compared with other methods on the basis of number of decomposed rectangles and time complexity. We use three measures to compare the performance of four methods.

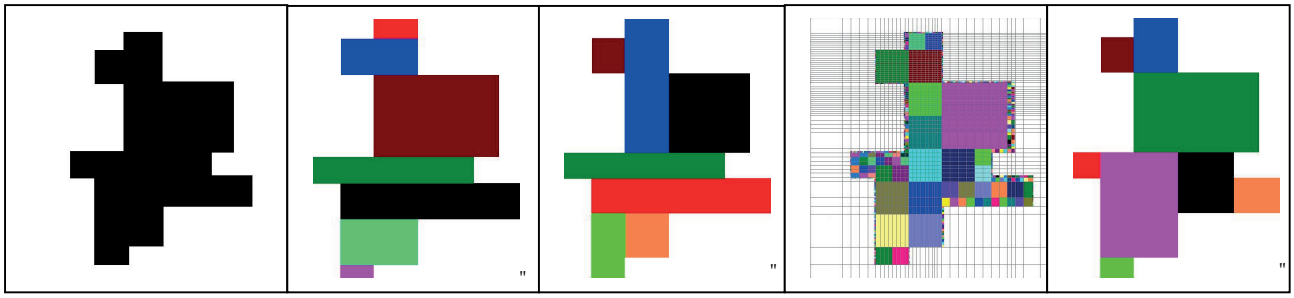

Figure 8. a) The image and its decomposition using b) GDM, c) GBD, d) QTD, e) proposed technique.

Number of Blocks: The number of blocks is the number of rectangle/square decomposed blocks that cover the compound shape.

Percentage Error: The percentage error with respect to perimeter (PEP) is defined as $PEP = \frac{|P_0 - P_D|}{P_0} \times 100$, where P_0 and P_D are the perimeters of the original object and the sum of the perimeters of the decomposed objects, respectively.

Run Time: Time taken by the algorithm to perform the decomposition task for the test image (satellite imagery). The I/O time was excluded from this measure. In this paper we have tested the performance of the proposed algorithm with other reported algorithms. Table 1 summarizes the performance of the four algorithms for the image shown in Figure 8. The results show that both GBD and GDM decomposition techniques performed the decomposition with the fewest blocks, although the proposed technique also used almost the same number of blocks. In contrast, the QTD decomposition technique produces the highest number of blocks. The minimum value of PEP was achieved by the GBD decomposition technique. The PEP value (percentage error) of the proposed technique is smaller than that of the other two techniques. In terms of computational time, our algorithm is at least an order of magnitude faster than the other algorithms. There are 9 and 10 buildings identified in Area 1 (Figure 7d) and Area 2 (Figure 7e), respectively, of Figure 7. Table 2 shows the performance of the four algorithms and the PEP values are less in maximum buildings of both areas by the proposed algorithm.

Table 1. The number of blocks, PEP and decomposition time achieved on the Figure 8.

Method	Number of blocks	PEP (%)	Time (s)	Complexity
GDM	7	68.4	5.8	O(p*q)
GBD	7	10.5	23.4	O(p*q)
QTD	448	282.08	38.7	$O(p*q)\log_4(p*q)$
Proposed method	8	15.08	1.9	O(p*q)

Table 2. The number of blocks and PEP(%) achieved on the Figure 7.

Method/ Object	GDM (Number of blocks/PEP (%))	GBD (Number of blocks/PEP (%))	QTD (Number of blocks/PEP (%))	Proposed method (Number of blocks/PEP (%))
Object 1 of Area 1	3/55.7	3/55.7	20/178.2	3/52.7
Object 2 of Area 1	2/30.3	2/25.8	22/145.1	2/23.2
Object 3 of Area 1	4/19.4	4/12.2	80/243.6	4/14.4
Object 4 of Area 1	4/6.7	3/4.1	25/167.8	4/4.3
Object 5 of Area 1	3/28.3	3/25.2	30/110.1	3/23.6
Object 6 of Area 1	3/75.3	2/70.3	45/213.5	3/71.2
Object 7 of Area 1	2/95.5	2/95.8	15/241.7	2/92.6
Object 8 of Area 1	2/30.1	2/24.2	25/256.2	2/24.1
Object 9 of Area 1	9/57.9	8/60.9	175/324.8	9/63.1
Object 1 of Area 2	2/25.5	2/25.1	12/136.3	2/24.3
Object 2 of Area 2	3/17.2	3/17.4	22/289.6	3/16.8
Object 3 of Area 2	2/19.4	2/19.3	13/158.1	2/18.7
Object 4 of Area 2	2/28.8	2/28.8	17/274.8	2/28.1
Object 5 of Area 2	7/57.2	7/51.6	248/462.3	8/52.2
Object 6 of Area 2	2/65.7	2/65.4	28/173.4	2/65.4
Object 7 of Area 2	2/40.4	2/40.2	46/249.4	2/40.6
Object 8 of Area 2	10/27.1	9/22.4	280/373.7	11/21.8
Object 9 of Area 2	10/14.6	9/12.9	170/193.1	10/12.1
Object 10 of Area 2	6/95.3	6/95.1	58/632.2	6/93.9

6. Summary

Decomposition of compound rectilinear objects is an important step in many applications including extraction of buildings from high-resolution satellite imagery since they manifest as compound rectilinear objects. In this paper, a method for decomposition of a compound rectilinear object into a minimal set of simple rectilinear objects has been presented. The decomposition technique begins with the accurate identification of the interior and exterior corner points of the compound rectilinear object. Guided by these corner points, the algorithm decomposes the compound rectilinear object into a set of disjoint rectilinear objects so that the difference between the perimeter of the compound rectilinear object and the sum of the lengths of the decomposed rectilinear objects is minimized. We have also proposed a modified corner point detection (MCPD) algorithm based on polygon approximation to handle objects with distorted boundaries. Results from a variety of domains

show that the proposed approach is both accurate and efficient. In addition, the proposed algorithm shows overall superior performance over algorithms in the literature in terms of percentage error with respect to perimeter and computational cost. Our future work includes the development of algorithms to identify buildings from panchromatic high-resolution satellite imagery from the results of the proposed algorithms in this paper.

References

[1] Zakaria MF, Vroomen LJ, Zsombor-Murray P, Vankessel JM. Fast algorithm for the computation of moment invariants. Pattern Recog 1987; 20: 639-643.

[2] Spiliotis IM, Mertzios BG. Real-time computation of two-dimensional moments on binary images using image block representation. IEEE T Image Process 1998; 7: 1609-1615.

[3] Kawaguchi E, Endo T. On a method of binary picture representation and its application to data compression. IEEE T Pattern Anal 1980; 29: 27-35.

[4] Keil JM. Polygon decomposition. In: Sack JR, Urrutia J, editors. Handbook of Computational Geometry. New York, NY, USA: Elsevier 2000. pp. 491-518.

[5] Zhang D, Lu G. Review of shape representation and description techniques. Pattern Recogn 2004; 37: 1-19.

[6] Wang H, Zhang W, Chen Y, Chen M, Yan K. Semantic decomposition and reconstruction of compound buildings with Semantic roofs from LiDAR data and Aerial imagery. Remote Sens-Basel 2015; 7: 13945-13974.

[7] Har-Peled S, Roy S. Approximating the maximum overlap of polygons under translation. Lecture Notes in Computer Science 2014; 6737: 542-553.

[8] Nagamochi H, Abe Y. An approximation algorithm for dissecting a rectangle into rectangles with specified areas. Discrete Appl Math 2007; 155: 523-537.

[9] Liu G, Xi Z, Lien JM. Dual space decomposition of 2D complex shapes. IEEE Conference on Computer Vision and Pattern recognition; 23-28 June 2014; Columbus, OH, USA: pp. 4154-4161.

[10] Patel TP, Panchal SR. Corner detection techniques: an introductory survey. Int. Journal of Engineering Development and Research 2014; 2: 3680-3686.

[11] Sojka E. A new algorithm for detecting corners in digital images. Proc. Spring Conference on Computer Graphics; 24–27 Apr 2002; Budmerice, Slovakia: pp. 55-62.

[12] Parvez MT, Mahmoud SA. Polygonal approximation of digital planar curves through adaptive optimizations. Pattern Recogn Lett 2010; 31: 1997-2005.

[13] Chaudhuri D, Kushwaha NK. Least square based automatic threshold selection for polygonal approximation of digital curves. International Journal of Advanced Technology & Engineering Research 2013; 3: 125-135.

[14] Song Y, Shan J. Building extraction from high resolution color imagery based on edge flow driven active contour and JSEG. In: The International Archives of the Photogrammetry, Remote Sensing and Spatial Information Sciences. XXXVII, Part B 3G; 3–11 July 2008; Bejing China: pp. 185-190.

[15] Rottensteiner F, Sohn G, Jung J, Gerke N, Baillard C, Benitez S, Breitkopf U. The ISPRS benchmark on urban object classification and 3D building reconstruction. Int Soc Photogramm 2012; 1: 293-298.

[16] Cramer M. The DGPF test on digital aerial camera evaluation - overview and test design. Photogramm Femerkun 2010; 2: 73-82.

[17] Chaudhuri D, Kushwaha NK, Samal A. Automatic building detection from high resolution satellite image based on morphology and internal gray energy operations. IEEE J Sel Top Appl 2016; 9: 1767-1779.